Talanta 232 (2021) 122396

Contents lists available at ScienceDirect

Talanta

journal homepage: www.elsevier.com/locate/talanta

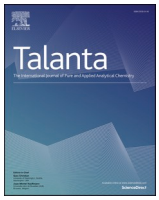

Microfluidic circulating reactor system for sensitive and automated duplex-specific nuclease-mediated microRNA detection

Xin Zhou [a], Hongmei Cao [b], Yong Zeng [a,c,*]

[a] Department of Chemistry, University of Florida, Gainesville, FL, 32611, USA
[b] Department of Chemistry, University of Kansas, Lawrence, KS, 66045, USA
[c] University of Florida Health Cancer Center, Gainesville, FL, 32610, USA

ARTICLE INFO

Keywords:
Duplex-specific nuclease
MicroRNA
Microfluidics
Biomarker

ABSTRACT

Duplex-specific nuclease signal amplification (DSNSA) is a promising microRNA (miRNA) quantification strategy. However, existing DSNSA based miRNA detection methods suffer from costly chemical consumptions and require laborious multi-step sample pretreatment that are prone to sample loss and contamination, including total RNA extraction and enrichment. To address these problems, herein we devised a pneumatically automated microfluidic reactor device that integrates both analyte extraction/enrichment and DSNSA-mediated miRNA detection in one streamlined analysis workflow. Two flow circulation strategies were investigated to determine the effects of flow conditions on the kinetics of on-chip DSNSA reaction in a bead-packed microreactor. With the optimized workflow, we demonstrated rapid, robust on-chip detection of miR-21 with a limit-of-detection of 35 amol, while greatly reducing the consumption of DSN enzyme to 0.1 U per assay. Therefore, this microfluidic system provides a useful tool for many applications, including clinical diagnosis.

1. Introduction

MicroRNAs (miRNA) are small non-coding RNAs that regulate gene expression [1] and have been found stable in RNase enriched environments, such as blood, urine, saliva, milk, and cerebrospinal fluid [2–5]. Due to these characteristics, miRNAs are promising biomarkers for a variety of diseases, such as diabetes [6], Alzheimer's disease [4,7], and cancer [8,9]. However, the detection of miRNAs in body fluid is challenging due to the low abundance of miRNAs [10]. The most commonly used methods to detect miRNAs are qRT-PCR [11–13] and RNA microarray [14–16]. As the gold standard of miRNA detection, qRT-PCR is highly sensitive with a limit of detection at the level of a few copies per microliter; but it usually requests tedious sample processing to remove inhibitory species and costly instrumentation. RNA microarray is a high throughput method that can analyze multiple targets of miRNAs, but its sensitivity is relatively lower. There is still an urgent need of a low-cost, sensitive and easy-to-use miRNA detection methods for biomedical applications, such as clinical diagnosis.

Recently, duplex-specific nuclease (DSN) has emerged as a new tool to develop simple and robust bioassays for miRNA quantitation because of its unique DNase activity that selectively cleaves double-strand DNA (dsDNA) or the DNA strand in a DNA-RNA hybrid, as opposed to single-strand DNA (ssDNA) or RNAs [17]. Based on this characteristic of the DSN, a numbers of DSN-mediated signal amplification (DSNSA) miRNA detection methods have been reported. For instance, an in-solution DSNSA-mediated miRNA detection assay that used a Taqman probe tagged with a fluorophore on one end and a quencher on the other end [18]. When hybridized with the target miRNA, the DNA probe is cleaved by DSN to separate the fluorescent dye from the quencher, generating the fluorescence signal. The released miRNA templates that can be recycled for another cycle of hybridization and DSN cleavage, and this process can be repeated thousands of times, leading to significant amplification in signal to improve the sensitivity of miRNA detection. Similarly, gold-nanoparticle (AuNP) labeled fluorescent ssDNA can also be applied as the capture probe during the DSNSA process [19]. The fluorophore attached on the ssDNA capture probe remained quenched by the surface of the AuNP until the ssDNA hybridized with the target miRNA and was cleaved by DSN. In addition, DSNSA based miRNA assays can also be achieved by immobilizing the fluorescently labeled ssDNA capture probe onto solid surfaces. For instance, magnetic beads-conjugated quantum dot-capped DNA capture probes (QD–CPs) were utilized to capture the target miRNA in a DSNSA-mediated miRNA assay for the purpose of Dengue virus detection [20]. After the DSNSA reaction, the beads carrying un-reacted capture probes were removed,

* Corresponding author. Department of Chemistry, University of Florida, Gainesville, FL, 32611, USA.
E-mail address: zengy@ufl.edu (Y. Zeng).

https://doi.org/10.1016/j.talanta.2021.122396
Received 22 February 2021; Received in revised form 31 March 2021; Accepted 1 April 2021
Available online 20 April 2021

and the supernatant is measured to quantify the intensity of released quantum dots. In contrast to standard PCR detection of miRNAs, these DSN-based isothermal methods enable direct detection of RNA fragments without the reverse transcription step, ease the design of specific primer/probes for short miRNA sequences, and negates the need for sophisticated thermal cycling instruments. Therefore, DSNSA is well poised for miRNA sensing because it simplifies the assay development, improves the assay robustness, mitigates the problems of sample degradation and contaminations, and reduces the assay cost. Despite these compelling advantages, the widespread application of DSNSA methods has been hampered by some practical barriers, such as the relatively high cost of DSN and lengthy enzymatic reaction required to afford high sensitivity due to the linear amplification process. To address these limitations, DSNSA has been coupled with other signal amplification mechanisms to enhance the sensitivity and shorten the assay time [21–23]. However, these multi-stage signal amplification methods involve complex reagent composition and assay protocols that need to be carefully optimized, which compromises the simplicity and robustness of DSN-based assays.

Herein, we attempted to exploit the microfluidic principles to develop a simple and rapid DSNSA-mediated miRNA detection system. Microfluidics has been broadly applied to bioanalysis because of its ability to improve detection sensitivity and analysis speed while reducing the consumption of sample and reagents [24–26]. It provides a platform that is capable of integrating multiple functions, such as sampling, sample enrichment, and detection all in one device by manipulating nanoliters to femtoliters of fluids in microchannels [27]. To date, many microfluidic platforms have been reported for miRNA detection using various assays, including RT-qPCR [28], digital PCR [29], RCA [30,31], ddPCR [32], and the hybridization assays coupled with encoded hydrogel particles [33–35], enzymatic amplification [36], laminar flow-assisted dendritic amplification [37,38], and electrochemical detection [39]. In addition, most of these microfluidic miRNA methods are capable of processing crude samples, such as cell lysate [31,33], human serum [35], without the need of off-chip RNA extraction. Despite the apparent advantages of microfluidics, very limited progress has been reported to date towards leveraging DSN-based miRNA detection. To our best knowledge, there have been only few reports on combining microfluidics with DSNSA for miRNAs detection. In one approach, the DSNSA assay was conducted in the conventional format and the microfluidic device was employed only as the ionization source for mass spectrometric analysis of the products of the DSN reaction [40]. The other report implemented the DSNSA detection strategy in an previously established self-priming microfluidic chip [41]. In contrast to these two methods, our system reported here directly adapts the microfluidic reaction and reagent manipulation to promote the performance of DSNSA for miRNA detection.

Our DSNSA-mediated microfluidic miRNA detection system integrates an affinity bead-packed microreactor for on-chip sample enrichment and purification and a pneumatically controlled microchannel circuit for DSNSA based miRNA detection. Solid-phase affinity capture using various materials, including magnetic beads [42], micro/nanostructures [43], hydrogel matrix [44], and agarose beads [45], affords an effective means for sample enrichment or signal enhancing. Compared to other surface-based systems, hydrogel particles offer from a number of advantages, such as 3D porous gel structure that provides enormous binding sites and the solution-like environment to promote binding kinetics [33–35], low cost, great biocompatibility, and robust chemistry for probe conjugation. Thus our miRNA detection system employs agarose beads for both target miRNA capture/enrichment and DSNSA-mediated miRNA detection. Using the pneumatically automated microreactor system, we investigated the sample flow rate for the solid-phase miRNA capture, studied DSNSA reaction at the circulating and oscillating-flow-control modes and optimized the assay protocol. As a proof-of-concept, we demonstrated on-chip detection of miR-21, which achieved a limit-of-detection (LOD) of 1.168 pM (35 amol) with ~1.5 h of sample enrichment and 2 h of DSNSA reaction. Compared to the off-chip assay, our on-chip DSNSA platform achieves significant improvement in sensitivity. Moreover, our method only consumes 0.1 U of DSN per assay, which is 1/6 of the amount of DSN needed for a 30 μL volume off-chip DSNSA miRNA assay, thus significantly reducing the cost. Overall, our microfluidic device provides a new method to improve the performance of DSNSA-mediated miRNA assays and thus can be useful for various applications, such as clinical diagnosis and point-of-care testing.

2. Experimental section

2.1. Chemical materials

All synthetic ssDNA and miRNA were purchased from Integrated DNA Technologies (IDT, Coralville, IA, USA). Sequences are listed in Table 1, respectively. HiTrap NHS-Activated HP affinity column was obtained from GE Healthcare (Chicago, IL, USA). Duplex-specific nuclease (DSN) is purchased from Evrogen (Moscow, Russia). Magnesium chloride (1 M) (Invitrogen), Ribolock RNase inhibitor (40 U/μL), Bovine Serum Albumin (BSA), 1 × Tris-EDTA solution, diethylpyrocarbonate (DEPC) treated water, Sodium chloride, Tris hydrochloride, and Tris-Base were ordered from Thermo Fisher Scientific (Waltham, MA, USA). Tween® 20 and ethanolamine were purchased from Sigma-Aldrich (St. Louis, MO, USA). 1 × Phosphate-Buffered Saline (PBS) was obtained from Mediatech, Inc. Sylgard® 184 Silicone Elastomer Kit is bought from Dow Corning Corporation (Midland, MI, USA).

2.2. Agarose bead modification

The fluorescent ssDNA capture probe was immobilized on 34 μm-diameter agarose beads via amine-NHS cross-linkage [46]. 0.1 g NHS activated Agarose beads were taken from the HiTrap NHS-Activated HP affinity columns and washed with cold 0.1 M HCl twice, cold water once, and cold 1 × PBS solution twice. The beads were then immerged into 400 μL 1 × PBS solution containing 6.6 μM probe ssDNA, mixing overnight on a rotator at room temperature. 0.5 M ethanolamine was used to block the active site on the beads surface by incubating for 2 h at room temperature the next day. The probe coated agarose beads were then washed with 1 × PBS solution containing 0.5 M NaCl three times and stored in 1 × TE buffer at 4 °C.

2.3. Microchip fabrication

The DSNSA circulation chip involves a Polydimethylsiloxane (PDMS) pneumatic control layer, a PDMS fluidic layer, and a glass substrate. Molds for both PDMS layers were fabricated by using standard photolithography on the 4″ silicon wafers (P100). The mold for the pneumatic layer of ~100 μm in height was patterned using SU-8 2050 (MicroChem). The mold for the fluidic layer underwent two-step photolithography process: a ~25 μm thick layer was spin coated first with SU-8 2025 (MicroChem) to pattern the flow channel and then the second ~75 μm thick layer of SU-8100 was coated and patterned to define the bead chamber and the detection window. Both of the molds were treated with a gas phase silanization with Trichloro(1H,1H,2H, 2H-perfluorooctyl) silane (Sigma Aldrich, St. Louis, MO, USA).

Table 1
Sequences of oligonucleotides.

Name	Sequence (5′–3′)
Capture probe for miR-21	5′-FAM-TCAACATCAGTCTGATAAGCTA–NH_2–3′
hsa-let-7a-5p	5′-UGAGGUAGUAGGUUGUAUAGUU-3′
hsa-miR-21-5p	5′-UAGCUUAUCAGACUGAUGUUGA-3′
hsa-miR-200a-3p	5′-UAACACUGUCUGGUAACGAUGU-3′
hsa-miR-200b-3p	5′-UAAUACUGCCUGGUAAUGAUGA-3′

Standard soft lithography was used for fabricating the pneumatic control layer and the fluidic layer. 40.5 g mixture of Sylgard® 184 at 8:1 (base: curing agent) weight ratio was poured onto the mold and incubated at 65 °C for 2 h. Once PDMS was cured on the mold, it was peeled off and cut into pieces. 1 mm diameter holes were punched as the inlet of each pneumatic control channel. 6 g mixture of Sylgard® 184 at a 15:1 (base: curing agent) weight ratio was spanned on the fluidic layer mold at 500 rpm for 30 s and 800 rpm for 30 s, followed with 2 h incubation at 65 °C for 2 h. The pneumatic control layer and the fluidic layer were treated with UV-ozone, then aligned and assembled manually. The assembled double-layer PDMS chip was incubated at 80 °C overnight for permanent bonding. After tearing the double layer chip off from the mold, a 2 mm diameter puncher was used to punch holes for inlets and outlets of each flow channel. The glass subtract was treated with piranha solution for 15 min before assembled with the double layer PDMS slab. UV-ozone was used to form permanent bonding between the glass slide and the PDMS slab. All flow channels were blocked with 0.1% BSA for at least 2 h. The chip was then stored at 4 °C until usage.

2.4. Off-chip DSNSA assay for off-chip optimization

The DSNSA assay was optimized in 0.5 ml reaction tubes before integrated into the chip. For the final optimum condition, 3 μL stock fluorescent ssDNA capture probe conjugated agarose beads were taken and washed with 50 mM Tris buffer (pH 8.0). The supernatant was then replaced by 29 μL of working solution (50 mM Tris buffer containing 10 mM $MgCl_2$, 0.8 U μL^{-1} RNase inhibitor, 0.02 U μL^{-1} DSN, pH 8.0). 1 μL miRNA was added to the solution as the analyte. The final reaction volume was 30 μL. The reaction tube was then rotated for 2 h at 40 °C in an incubator (Benchmark Scientific, NJ, USA). After the reaction, the fluorescence intensity of the supernatant was measure by Biotek Cytation 5 imaging reader (Biotek, VT, USA).

2.5. On-chip DSNSA assay

Before the assay, all the chip channels were washed with DEPC-treated water, and then the probe conjugated agarose beads were filled into the bead chamber by gravity. The solution in each channel was replaced by the capture buffer (1 × TE buffer containing 350 mM NaCl and 0.05% (w/v) Tween®20) [34]. Right before the capture, the chip was placed on a hotplate at 95 °C for 5 min and then cooled down to 0 °C on ice. The on-chip pumping then started to pump the buffer flowing through the beads. During the capture process, at room temperature, 30 μL of sample in the capture buffer was pumping through the bead chamber at room temperature by using the on-chip 4-step pumping with a flow rate at 0.34 μL/min, followed with 5 μL capture buffer. Once the capture process was done, the on-chip pumping was stopped. For the DSNSA reaction, the buffer in all the channels was replaced with ice-cold working solution (50 mM Tris buffer containing 10 mM $MgCl_2$, 0.8 U μL^{-1} RNase inhibitor, 0.02 U μL^{-1} DSN, pH 8.0) by flushing each channel with 5 μL working solution. All the pneumatic valves were then closed, and the on-chip pumping was engaged to make the Agarose beads oscillate inside the bead chamber to enhance the mixing efficiency. The chip was placed at a 40 °C incubator for 2 h for the DSNSA reaction. After the reaction was finished, the fluorescence intensity of the detection chamber was tested using a fluorescence microscope. The image was analyzed using ImageJ (NIH).

2.6. qRT-PCR

Reverse transcription was done by using TaqMan™ MicroRNA Reverse Transcription Kit (Applied Biosystem, Foster City, CA, USA). The operation followed the manufacturer's protocol with slight changes. Briefly, each 30 μL reverse transcription reaction mix consists of 0.3 μL 100 mM dNTPs, 2 μL 50 U μL^{-1} MultiScribe™ Reverse Transcriptase, 3 μL 10 × Reverse Transcription Buffer, 0.38 μL 20 U μL^{-1} RNase inhibitor, 16.32 μL RNase free water, 6 μL 5 × RT primer and 2 μL RNA sample. The Reverse transcription mix was incubated at 16 °C for 30 min, 42 °C for 30 min, 85 °C for 5 min, and ended at 4 °C. qPCR was done by using the TaqMan® MicroRNA assay (Applied Biosystem, Foster City, CA, USA) on Mastercycler epgradient S (Eppendorf). Each 20 μL PCR mix consists of 1 μL 20 × TaqMan MicroRNA Assay, 1.33 μL RT reaction product, 10 μL TaqMan 2 × Universal PCR Master Mix (No AmpErase UNG), and 7.67 μL Nuclease-free water. The PCR mix was incubated at 95 °C for 10 min, 40 cycles of 95 °C denature for 15 s and 60 °C anneal/extend for 60 s. For testing the biological sample, 1 mg/mL Breast Adenocarcinoma (MCF-7) total RNA (Invitrogen, Carlsbad, CA, USA) was diluted to 1 ng/uL and 10 ng/uL with nuclease-free water, and then analyzed by using the qRT-PCR protocol described above. The result was compared with the data from the On-Chip DSNSA assay.

3. Results and discussion

3.1. Chip design and assay principle

The principle of our method is to utilize the microfluidic reaction system to promote the DSN enzymatic reaction while reducing the amount of expensive DSN enzyme needed. To further enhance the analytical sensitivity and speed, we intended to construct a total analytical system that combines sample processing (i.e., isolation and enrichment of specific miRNAs from biological samples) and miRNA quantification by DSNSA assay in one on-chip workflow. This capacity would enable direct miRNA detection without the need of total RNA purification which may result in variability in yield, sequence bias, cross contaminations, and RNA degradation [31,47]. A photo and the design of our microfluidic chip that contains three units were shown in Fig. 1A and B, respectively. It is a multi-layer device that consists of a PDMS pneumatic control layer, a PDMS fluidic layer, and a glass substrate. In the pneumatic control layer, the control circuit designed for precise delivery and routing of samples/reagents consists of a three-valve pump [48] and a set of lifting-gate valves [49] that control the input reservoir, output reservoir and circulation channel, respectively. The fluidic layer contains a main flow channel connecting a bead-packed microchamber and a detection chamber, as well as a circulation channel. The flow channels and the microchamber were fabricated to be ~25 μm and ~100 μm in height to trap DNA probe-conjugated agarose beads of ~34 μm in average diameter in the bead chamber for on-chip sample enrichment and DSNSA reaction (Fig. 1B(a)). The width of the flow channel and the bead chamber are 150 μm and 1500 μm, respectively. A detection chamber of 100 μm in height and 450 μm in width is incorporated downstream to avoid the signal interference from the fluorescent agarose beads. Compared to the 25 μm-high flow channels, this tall detection chamber provides a four-fold optical distance, which greatly enhances the sensitivity of fluorescence detection as shown in Fig. 1B(b).

The on-chip miRNA assay workflow, as illustrated in Fig. 1C, consists of three steps: solid-phase miRNA capture step, DSNSA reaction, and fluorescence detection. In the miRNA capture step, the sample solution was driven by the 4-step on-chip pumping to flow through the bead-packed chamber. The target miRNA is captured and enriched by the complementary ssDNA capture probe immobilized on the agarose beads. The DSNSA-reaction step is then carried out after replacing the buffer in the channel with the reaction master mix and increasing the temperature. The DSNSA reaction relies on the nature of duplex-specific nuclease (DSN), which only hydrolyzes the DNA part of a DNA-miRNA hybrid and thus releases the miRNA. The released miRNA is subsequently captured by another probe and form a DNA-miRNA hybrid again, ready for the next cleavage. Meanwhile, the fluorophore attached to the probe DNA strand is also released to serve as the source of the signal. The on-chip pumping keeps working using the same parameter set as in the capture step, during which the reaction system is sealed by closing both input and output valves to avoid the diffusion toward the inlet and outlet reservoirs. As shown in the supplementary Video 1, the

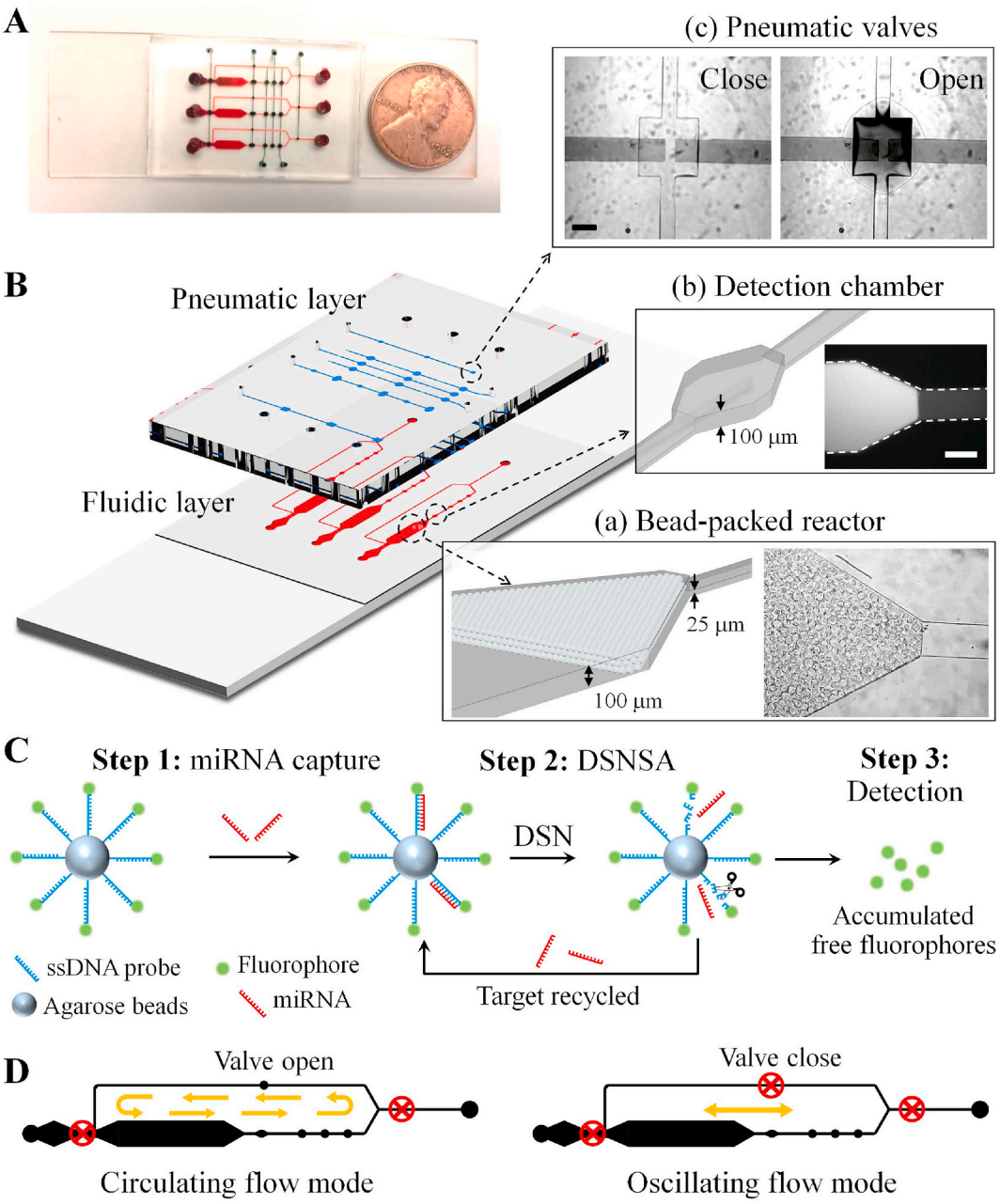

Fig. 1. Automated microfluidic system for DSNSA-mediated miRNA detection. (A) Photo of a pneumatically automated microfluidic circulating chip with red dye filled in the bottom flow channels and green dye filled in the top pneumatic control circuit. (B) Design of the chip showing the pneumatic control layer, the fluidic layer and the glass substrate. (a) Drawing (left) and white-field image (right) of the microchamber to trap agarose beads for DSNSA reaction. (b) Drawing (left) and fluorescence image (right) of the detection chamber to enhance fluorescence signal intensity. (c) White-field images of a lift-gate valve operated to control flow direction. Scale bars: 150 μm. (C) Schematic of the integrated on-chip DSNSA miRNA assay workflow: (1) Solid-phase miRNA capture by flowing the sample through the bead-packed microchamber. (2) DSNSA reaction step, during which the fluorescent ssDNA capture probes of the DNA-RNA hybrids are cleaved by DSN to release the fluorophore and the miRNA. The capture and cleavage cycle repeats until the end of this step. (3) The accumulated free fluorophore is then measured to determine the concentration of the analyte miRNA. (D) Schematic of the circulating-flow mode and the oscillating-flow mode designed for improving the flow mixing during the DSNSA reaction. (For interpretation of the references to colour in this figure legend, the reader is referred to the Web version of this article.)

reaction system is being stirred thoroughly by the on-chip pumping to expedite the DSNSA reaction. In the meantime, the released fluorophore molecules are defusing homogenously to all channels, including the detection chamber for the signal readout. The design of the circulation channel and the circulation valve (Fig. 1B(c)) allow us to assess two different flow control modes in order to optimize the on-chip DSNSA reaction. As depicted in Fig. 1D, the circulating-flow mode allows the reaction mixture except the agarose beads to flow along the channel circuit as the circulation valve is open. In contract, in the oscillating-flow mode, the circulation valve is closed and the micropump was operated to oscillate the reaction mixture within the main channel.

Supplementary data related to this article can be found online at https://doi.org/10.1016/j.talanta.2021.122396

3.2. Agarose bead-based DSNSA miRNA assay

Although the reaction parameters of the DSNSA reaction were well established in previous studies, the DSNSA on agarose surface has not

been studied yet. We selected miR-21 as the analyte for the development of our assay. The miR-21 is a promising biomarker associated with a variety of cancers, including breast cancer [50], lung cancer [51,52], prostate cancer [53], pancreatic cancer [54], colon cancer [55], gastric cancer [56], etc. It is essential and meaningful to detect miR-21 rapidly, sensitively, and cost-effectively. To simplify the development of our on-chip DSNSA method, the optimization of reaction parameters, such as the concentration of $MgCl_2$ and the reaction temperature, was carried on via off-chip DSNSA assays.

The concentration of $MgCl_2$ was optimized in reaction tubes due to the fact that the enzymatic activity of DSN can be impacted by the concentration of the Mg^{2+} ion in the reaction system. Interestingly, as presented in Fig. 2A, it was observed that the signal intensity was increasing along with the $MgCl_2$ concentration until 10 mM and then decreasing. This could be a result of the decrease in the DSN activity due to the increasing ionic strength [17]. Thus, 10 mM was picked as the optimum $MgCl_2$ concentration for our on-chip DSNSA assay. The reaction temperature was also investigated since it is an important parameter that determines the reaction rate of the DSN enzymatic reaction. We optimized the reaction temperature by performing the DSN reaction under different temperatures in the range from 30 to 60 °C in reaction tubes. As depicted in Fig. 2B, the signal intensity reached the highest value at 40 °C and then dropped rapidly, while the reported working temperature of DSN could be as high as 60 °C [17]. This could be caused by the melting DNA-miRNA hybrids at the high temperature due to the low melting temperature of miRNA. Therefore, 40 °C was determined to be the best working condition for the DSNSA reaction.

However, the off-chip DSNSA miRNA assay is not cost-effective due to its need for a large amount of DSN per each assay. On the other hand, there is still room to improve the sensitivity due to the inefficient mixing of the beads and the fluid during the DSNSA reaction. As demonstrated in Fig. 2C, with our microfluidic device, a much higher signal was obtained while a lower background was achieved. This was due to the higher surface-to-volume ratio in the micrometer scale microfluidic channel than that in a centrifuge tube. Meanwhile, the pumping system build in the chip also provides an efficient mixing for the reaction system, which expedited the DSNSA reaction.

3.3. Microfluidic DSNSA

The optimized DSNSA mediated miRNA assay was employed on the microfluidic platform, on which the fluorescence signal could be measured at the detection chamber, as demonstrated in Fig. 3A. A solid-phase miRNA capture step was integrated into the on-chip assay prior to the DSNSA reaction. In the capture step, the flow rate of the sample solution is an important parameter that significantly influences the sample capture efficiency [57]. A high flow rate will shorten the capture time, but it will also reduce the interaction between the target miRNA molecules and the ssDNA capture probes, resulting in a decrease of capture efficiency. In our chip, the flow rate can be controlled by employing different pumping parameter sets for the on-chip pump, as described previously [48]. To optimize the flow rate for the sample capture step, we tested 0.14, 0.34, 0.43, 0.60, 0.83 μL/min as the flow rate of 30 μL of 500 pM miR-21, followed with on-chip DSNSA detection with the same reaction condition. As shown in Fig. 3B, flow rates higher than 0.34 μL/min caused signal dropping, which indicated insufficient capture efficiency. Interestingly, a slower flow rate also leads to signal reduction, presumably attributed to the degradation of miRNA when held at room temperature for too long. Hence, 0.34 μL/min was selected to be the optimum flow rate for the on-chip sample capture process. For

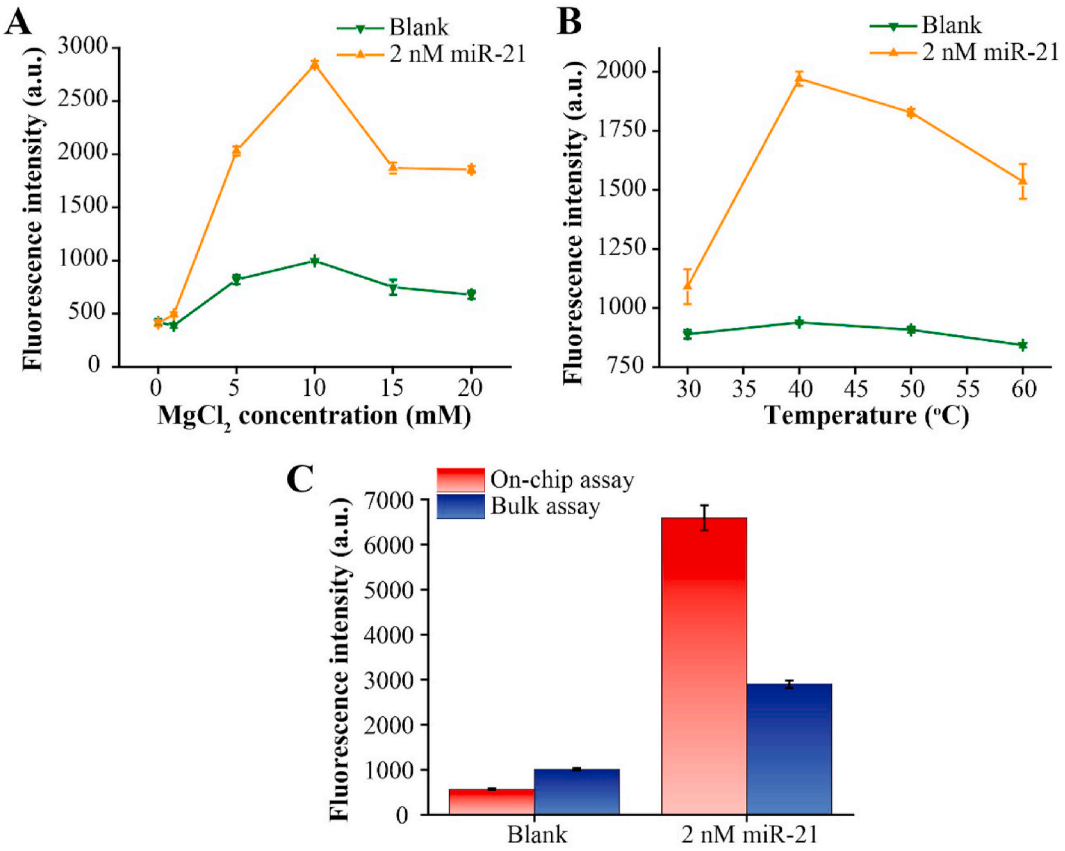

Fig. 2. Development of agarose bead-based DSNSA. (A) Optimization of $MgCl_2$ concentration. (B) Optimization of reaction temperature. (C) Comparison between the signal detected for the on-chip assay and the bulk assay for miRNA detection. The on-chip approach was performed with the circulating flow mode during the on-chip DSNSA process. Error bars: standard deviation (n = 3).

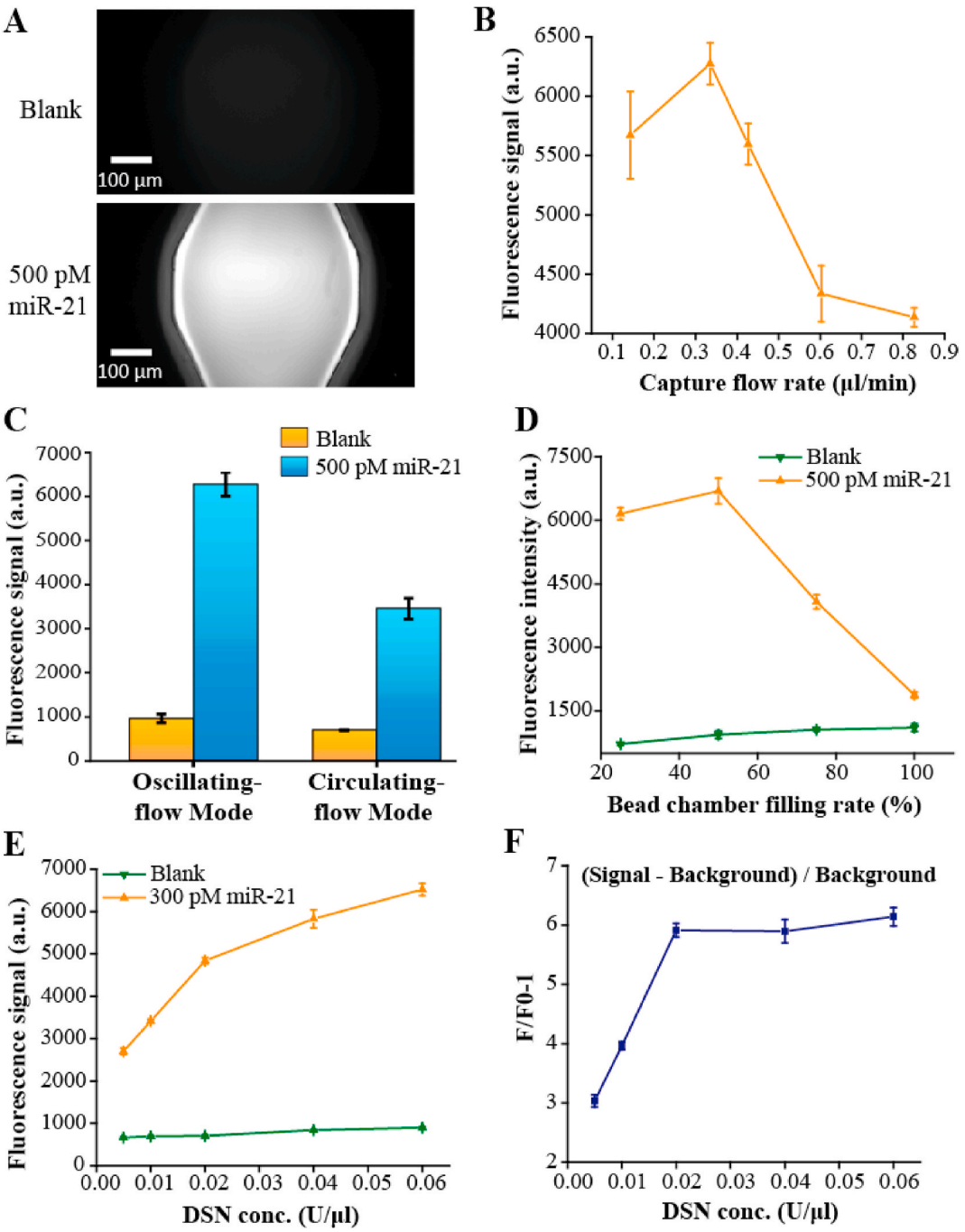

Fig. 3. On-chip DSNSA assay optimization. (A) Fluorescence images taken at the detection chamber after the on-chip DSNSA assay with the blank and 500 pM miR-21. (B) Optimization of the sample flow rate used in the solid-phase miRNA capture step. (C) Signal comparison between the oscillating flow mode and the circulating flow mode for the DSNSA reaction. (D) Comparison of signal intensity of 300 pM miR-21 and blank with different beads amount. (E) Optimization of DSN concentration using 300 pM miR-21 and blank. (F) Background subtraction for optimization of DSN concentration shown in (E). Error bars: standard deviation (n = 3).

30 μL of the sample solution, it required less than 1.5 h to finish the capture step.

In order to achieve a satisfactory sensitivity, the on-chip DSNSA assay requires a thorough mixing of the system during the reaction. However, most of the existing on-chip mixers, such as stagger herring-bone mixer [58], twisted channel [59], zigzag channels [60], etc., are designed for continuous flow. Although some of the mixers are able to mix the reaction system locally, they require sophisticated acoustic-activation technology [61,62], which may cause a rise of temperature due to ultrasonic irradiation and thus not ideal for the on-chip DSNSA assay. To address the need for a simple local mixer for the on-chip DSNSA assay, we designed an active mixing strategy by taking advantage of the pneumatic-controlled on-chip pumping. To study the impact of different flow types on the on-chip DSNSA assay, we designed a circulation channel and a circulation valve to enable the circulating-flow-control mode and the oscillating-flow-control mode, as above mentioned. The on-chip pump kept working with the same parameter set for both mixing modes, but the reaction system was mixed in a different way according to the status of the circulation valve, as illustrated in Fig. 1D. The circulating flow mode mixed the reaction system with the continuous flow, while the oscillating flow mode does that with locally mixing. To determine the optimum mixing strategy for

the on-chip DSNSA assay, we compared these two mixing modes by analyzing 30 μL 500 mM miR-21. As shown in Fig. 3C, it was notably the signal of 500 pM miR-21 from the oscillating flow mode was almost as twice as that from the circulating flowing mode, while the background remained nearly unchanged. The relatively lower mixing efficiency of the circulating-flow-control mode could be explained by the lack of contact between the miRNA and the probe-conjugated agarose beads when the released miRNA molecules were flowing in the circulation channel. With the circulating-flow-control, each molecule of target miRNA needs to travel along the circulation loop channel after being released from the capture probe by DSN to return to the beads chamber to be capture again. However, there is no DSNSA reaction happening inside the circulation loop channel, so the travel of each target miRNA inside the circulation loop did not contribute to the signal generation. Consequently, with the oscillating-flow-control mode, the target miRNA does not have to travel through the loop channel to be re-captured. Thus, in terms of the miRNA capture efficiency, the oscillating-flow-control mode performs way better than the circulating-flow-control mode and thus was picked as the optimum mixing strategy for the on-chip DSNSA reaction.

The amount of probe conjugated agarose beads filling in the beads chamber is significant to both the solid-phase miRNA capture step and the DSNSA-reaction step. More beads will provide more binding sites for the target miRNA capture, but could cause problems such as an increase of background. To determine the optimum beads amount filled into the chamber, we filled the chamber with different amounts of beads and performed the on-chip DSNSA assay on 30 μL of 500 pM miR-21. As illustrated in Fig. 3D, although the background went up as the amount of beads increased, the signal started to decrease when the beads fill out the chamber over 50%. This could be due to the reduced volume of the reaction master buffer within the channel caused by the increased space occupied by the agarose beads. Thus the total amount of DSN was not enough to maintain the enzymatic reaction rate, resulting in low efficient signal amplification. Therefore, filling the chamber 50% with the beads was chosen to be the best condition for the on-chip DSNSA miRNA assay.

The concentration of DSN is vital for the DSNSA reaction in terms of both assay sensitivity and reagent consumption. To optimize the DSN concentration, the on-chip DSNSA mediated miRNA assay was carried out on 30 μL of 300 pM miR-21 with five different DSN concentrations from 0.005 to 0.06 U μL^{-1}. As shown in Fig. 3E, although the signal of miRNA increased along with the rise of the DSN concentration, the background performed the same. To accurately evaluate the impact of different DSN concentrations, we subtracted the background as illustrated in Fig. 3F. It was evident that the signal reaches a platform after 0.02 U μL^{-1}, which indicated that a DSN concentration higher than 0.02 U μL^{-1} would not help to increase the sensitivity of this assay. Therefore, 0.02 U μL^{-1} was selected to be the optimum concentration of DSN for our on-chip DSNSA miRNA assay. With the optimum DSN concentration, our on-chip method only required 0.1U of DSN. Compared to the conventional off-chip DSNSA mediated miRNA assay that usually required at least 30 μL of working solution containing DSN, our on-chip strategy only needs 5 μL, significantly reducing the consumption of DSN per test.

Although the specificity of the DSNSA miRNA assay has been well studied in conventional off-chip platforms, it is still important to verify it on our microfluidic platform. To investigate the specificity of the on-chip DSNSA mediated miRNA assay, high concentration (1 nM) of Let7a, Let7b, miR-200a, and miR-200 b were measured by using the

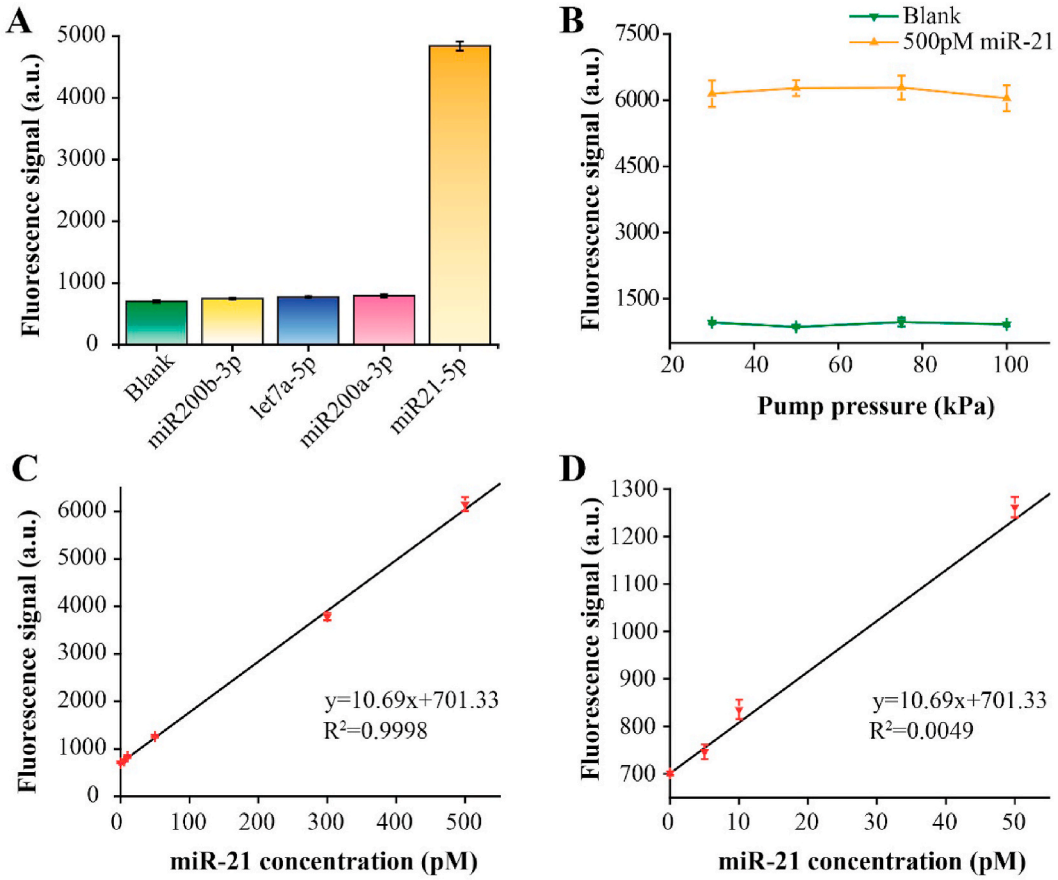

Fig. 4. Analytical performance of the microfluidic DSNSA mediated miR-21 assay. (A) Specificity test of on-chip DSNSA miR-21 assay. (B) Signal intensity comparison of 500 pM miR-21 and the blank using different pumping pressure during the reaction step. (C) Calibration curve of miR-21 detection using the microfluidic DSNSA. (D) Expanded view of the low concentration range of the plot in (C). Error bars: standard deviation (n = 3).

miR-21 probe, respectively. As depicted in Fig. 4A, the signal intensities of these high concentrated non-target miRNAs from the assay were all at blank level, while only 300 pM of miR-21 obtained a fluorescence signal in high intensity, which indicated the specificity of the DSNSA mediated miRNA assay remained excellent on our on-chip platform.

Good reproducibility is essential for our approach when performed on different instruments, in which case the pump pressure applied to the pneumatic control circuit is the primary variable. To assess the reproducibility of our method, we performed the on-chip DSNSA assay on 30 μL of 500 pM miR-21 with diverse pump pressures from 30 kPa to 100 kPa. As shown in Fig. 4B, neither the signal intensity nor the blank level was significantly impacted by the change of pressure. This result revealed that our method was qualified with excellent reproducibility and capable of tolerating large variation of pump pressure that could possibly occur when performed on different instruments.

We calibrated the on-chip DSNSA mediated miRNA assay with synthetic miR-21 under the optimum reaction conditions. As illustrated in Fig. 4C, the linear range of our approach is from 5 to 500 pM. The correlation equation was $Y = 10.69X+701.33$ ($R^2 = 0.9998$), in which Y represents the fluorescence intensity observed at the detection chamber, and X represents the concentration of miR-21 in unit of pico-molar. A detection limit at 1.168 pM was obtained based on the summary of the value of blank signal and three standard deviations. Furthermore, a good linear relationship was retained even in the low concentration range (<50 pM), as shown in Fig. 4D. In addition, compared to the off-Chip assay, our on-chip platform achieved significant improvement in sensitivity, which is due to the increased surface-to-volume ratio enabled by the microfluidic platform, as well as the enhanced mixing efficiency assisted by the oscillating-flow-control mode. These results demonstrated that our microfluidic platform significantly increased the sensitivity of the DSNSA miRNA assay.

3.4. Testing with biological samples

To investigate the applicability of our on-chip DSNSA method on biological specimens, we measured the miR-21 in the total RNA extracted from a breast adenocarcinoma cell line MCF-7, and the commercial stem-loop RT-qPCR Taqman™ miRNA assay was employed as the validation. As shown in Fig. 5A, a calibration curve of miR-21 standard was prepared with the commercial RT-qPCR method for the purpose of quantitative measuring of miR-21 in the total RNA sample. For the quantitation of miR-21 in the total RNA extracted from MCF-7 cell line, 1 mg/ml extracted total RNA was diluted to 10 ng/μL and 1 ng/μL and measured by our on-chip approach and the commercial RT-qPCR method. As shown in Fig. 5B, the concentration of miR-21 in 10 ng/ml and 1 ng/ml of the total RNA measured by our on-chip DSNSA approach was 91.9 ± 2.62 pM and 10.99 ± 2.04 pM, respectively. These results matched that from the commercial RT-qPCR method, which were 95.92 ± 1.06 pM and 8.4 ± 1.08 pM, respectively. This suggests that our approach is capable of analyzing biological samples with high accuracy and robustness. In addition, compared to the standard RT-qPCR method, our on-chip method does not require a reverse transcription method and can process the sample within the chip with high level of automation. Such capability not only minimizes the human errors existing in the laboratory operation process, but also reduce the potential sample contamination and RNA degradation, thus holding great promise for its potential adaptability to a variety of applications, such as clinical diagnosis. Furthermore, it is possible to detect miRNAs directly in complex biofluids, such as blood plasma or serum [35]. Previous studies have demonstrated the superior performance of hydrogels for nucleic acid binding, especially from complex biological samples, compared to other solid-phase biosensing systems, due in part to the non-fouling nature of the hydrogels. Adapting our method to measurements of clinical biofluids will require further optimization of the assay parameters, such as the sample preheating which was found to suppress non-specific adsorption during the incubation step for target capture [33]. In addition, to further mitigate the potential cross-reactivity issue caused by the mismatch between the capture probes and interfering nucleic acids, we can increase the temperature for DSNSA reaction to ensure highly specific miRNA/probe hybridization, because the working temperature of DSN was reported to be as high as 60 °C.

4. Conclusion

We have successfully developed a low-cost, sensitive, and easy-to-use on-chip DSNSA-mediated assay for miRNA detection. Our method integrated the sample enrichment and the DSNSA mediated miRNA assay in one streamlined analysis workflow and obtained a LOD at 1.168 pM (35.04 amol) of miR-21 and a dynamic range from 5 to 500 pM with excellent specificity and robustness, only requiring 0.1 U DSN per test. As a proof-of-concept, we used our method to quantitatively measure the miR-21 in the total RNA extracted from the MCF-7 cell line, and the result was verified with the commercial stem-loop RT-qPCR Taqman™ miRNA assay. Our on-chip approach significantly improved the competitivity of the DSNSA miRNA assay. It thus potentially can be utilized in numerous fields, such as clinical diagnosis and point-of-care testing.

Credit author statement

Xin Zhou: Methodology, Data curation, Writing – original draft,

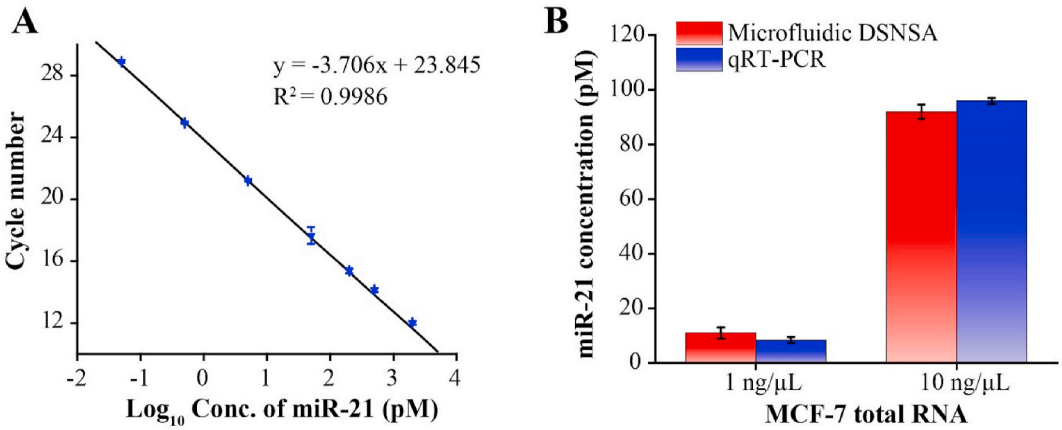

Fig. 5. Detection of miR-21 in MCF-7 total RNA with the microfluidic DSNSA assay and commercial RT-qPCR. (A) Calibration curve for qRT-PCR detection of miR-21. (B) Comparison of the measured miR-21 levels in the total RNA extraction from MCF-7 cell line at different concentrations using the microfluidic DSNSA and qRT-PCR. Error bars represent standard deviation (n = 3).

Investigation, Formal analysis, Visualization. **Hongmei Cao**: Investigation, Data curation, Validation. **Yong Zeng**: Conceptualization, Supervision, Resources, Visualization, Writing – review & editing, Funding acquisition.

Declaration of competing interest

The authors declare that they have no known competing financial interests or personal relationships that could have appeared to influence the work reported in this paper.

Acknowledge

This research was in part supported by the National Institutes of Health grants R21EB024101, R33CA214333, and R01CA243445.

References

[1] M.I. Almeida, R.M. Reis, G.A. Calin, MicroRNA history: discovery, recent applications, and next frontiers, Mutat. Res. 717 (2011) 1–8.
[2] A. Keller, P. Leidinger, A. Bauer, A. ElSharawy, J. Haas, C. Backes, A. Wendschlag, N. Giese, C. Tjaden, K. Ott, Toward the blood-borne miRNome of human diseases, Nat. Methods 8 (2011) 841.
[3] L.F. Sempere, Tissue slide-based microRNA characterization of tumors: how detailed could diagnosis become for cancer medicine? Expert Rev. Mol. Diagn. 14 (2014) 853–869.
[4] D. Galimberti, C. Villa, C. Fenoglio, M. Serpente, L. Ghezzi, S.M. Cioffi, A. Arighi, G. Fumagalli, E. Scarpini, Circulating miRNAs as potential biomarkers in Alzheimer's disease, J. Alzheimers Dis. 42 (2014) 1261–1267.
[5] J.A. Weber, D.H. Baxter, S. Zhang, D.Y. Huang, K. How Huang, M. Jen Lee, D. J. Galas, K. Wang, The microRNA spectrum in 12 body fluids, Clin. Chem. 56 (2010) 1733–1741.
[6] J. Feng, W. Xing, L. Xie, Regulatory roles of microRNAs in diabetes, Int. J. Mol. Sci. 17 (2016) 1729.
[7] G.D. Femminella, N. Ferrara, G. Rengo, The emerging role of microRNAs in Alzheimer's disease, Front. Physiol. 6 (2015) 40.
[8] T.A. Farazi, J.I. Spitzer, P. Morozov, T. Tuschl, miRNAs in human cancer, J. Pathol. 223 (2011) 102–115.
[9] G. Di Leva, C.M. Croce, miRNA profiling of cancer, Curr. Opin. Genet. Dev. 23 (2013) 3–11.
[10] P. Tiberio, M. Callari, V. Angeloni, M.G. Daidone, V. Appierto, Challenges in using circulating miRNAs as cancer biomarkers, BioMed Res. Int. 2015 (2015).
[11] C. Chen, D.A. Ridzon, A.J. Broomer, Z. Zhou, D.H. Lee, J.T. Nguyen, M. Barbisin, N. L. Xu, V.R. Mahuvakar, M.R. Andersen, Real-time quantification of microRNAs by stem–loop RT–PCR, Nucleic Acids Res. 33 (2005) e179-e179.
[12] V. Benes, M. Castoldi, Expression profiling of microRNA using real-time quantitative PCR, how to use it and what is available, Methods 50 (2010) 244–249.
[13] N. Redshaw, T. Wilkes, A. Whale, S. Cowen, J. Huggett, C.A. Foy, A comparison of miRNA isolation and RT-qPCR technologies and their effects on quantification accuracy and repeatability, Biotechniques 54 (2013) 155–164.
[14] U. Bissels, S. Wild, S. Tomiuk, A. Holste, M. Hafner, T. Tuschl, A. Bosio, Absolute quantification of microRNAs by using a universal reference, RNA 15 (2009) 2375–2384.
[15] A. Git, H. Dvinge, M. Salmon-Divon, M. Osborne, C. Kutter, J. Hadfield, P. Bertone, C. Caldas, Systematic comparison of microarray profiling, real-time PCR, and next-generation sequencing technologies for measuring differential microRNA expression, RNA 16 (2010) 991–1006.
[16] S.G. Jensen, P. Lamy, M.H. Rasmussen, M.S. Ostenfeld, L. Dyrskjøt, T.F. Ørntoft, C. L. Andersen, Evaluation of two commercial global miRNA expression profiling platforms for detection of less abundant miRNAs, BMC Genom. 12 (2011) 435.
[17] V.E. Anisimova, D.V. Rebrikov, D.A. Shagin, V.B. Kozhemyako, N.I. Menzorova, D. B. Staroverov, R. Ziganshin, L.L. Vagner, V.A. Rasskazov, S.A. Lukyanov, Isolation, characterization and molecular cloning of Duplex-Specific Nuclease from the hepatopancreas of the Kamchatka crab, BMC Biochem. 9 (2008) 14.
[18] B.-C. Yin, Y.-Q. Liu, B.-C. Ye, One-step, multiplexed fluorescence detection of microRNAs based on duplex-specific nuclease signal amplification, J. Am. Chem. Soc. 134 (2012) 5064–5067.
[19] F. Degliangeli, P. Kshirsagar, V. Brunetti, P.P. Pompa, R. Fiammengo, Absolute and direct microRNA quantification using DNA–gold nanoparticle probes, J. Am. Chem. Soc. 136 (2014) 2264–2267.
[20] W. Shen, Z. Gao, Quantum dots and duplex-specific nuclease enabled ultrasensitive detection and serotyping of Dengue viruses in one step in a single tube, Biosens. Bioelectron. 65 (2015) 327–332.
[21] L. Lu, B. Yang, T. Kang, A dual amplification strategy for ultrasensitive detection of microRNA, Appl. Surf. Sci. 426 (2017) 597–604.
[22] K. Zhang, K. Wang, X. Zhu, F. Xu, M. Xie, Sensitive detection of microRNA in complex biological samples by using two stages DSN-assisted target recycling signal amplification method, Biosens. Bioelectron. 87 (2017) 358–364.
[23] B. Bo, T. Zhang, Y. Jiang, H. Cui, P. Miao, Triple signal amplification strategy for ultrasensitive determination of MiRNA based on duplex specific nuclease and bridge DNA-gold nanoparticles, Anal. Chem. 90 (2018) 2395–2400.
[24] D.R. Reyes, D. Iossifidis, P.-A. Auroux, A. Manz, Micro total analysis systems. 1. Introduction, theory, and technology, Anal. Chem. 74 (2002) 2623–2636.
[25] P.S. Dittrich, K. Tachikawa, A. Manz, Micro total analysis systems. Latest advancements and trends, Anal. Chem. 78 (2006) 3887–3908.
[26] T. Vilkner, D. Janasek, A. Manz, Micro total analysis systems. Recent developments, Anal. Chem. 76 (2004) 3373–3386.
[27] Y. Zeng, T. Wang, Quantitative microfluidic biomolecular analysis for systems biology and medicine, Anal. Bioanal. Chem. 405 (2013) 5743–5758.
[28] A.K. White, M. VanInsberghe, I. Petriv, M. Hamidi, D. Sikorski, M.A. Marra, J. Piret, S. Aparicio, C.L. Hansen, High-throughput microfluidic single-cell RT-qPCR, Proc. Natl. Acad. Sci. Unit. States Am. 108 (2011) 13999–14004.
[29] A. White, K. Heyries, C. Doolin, M. Vaninsberghe, C. Hansen, High-throughput microfluidic single-cell digital polymerase chain reaction, Anal. Chem. 85 (2013) 7182–7190.
[30] K. Sato, A. Tachihara, B. Renberg, K. Mawatari, K. Sato, Y. Tanaka, J. Jarvius, M. Nilsson, T. Kitamori, Microbead-based rolling circle amplification in a microchip for sensitive DNA detection, Lab Chip 10 (2010) 1262–1266.
[31] H. Cao, X. Zhou, Y. Zeng, Microfluidic exponential rolling circle amplification for sensitive microRNA detection directly from biological samples, Sensor. Actuator. B Chem. 279 (2019) 447–457.
[32] K. Zhang, D.-K. Kang, M.M. Ali, L. Liu, L. Labanieh, M. Lu, H. Riazifar, T. N. Nguyen, J.A. Zell, M.A. Digman, Digital quantification of miRNA directly in plasma using integrated comprehensive droplet digital detection, Lab Chip 15 (2015) 4217–4226.
[33] H. Lee, S.J. Shapiro, S.C. Chapin, P.S. Doyle, Encoded hydrogel microparticles for sensitive and multiplex microRNA detection directly from raw cell lysates, Anal. Chem. 88 (2016) 3075–3081.
[34] S.C. Chapin, D.C. Appleyard, D.C. Pregibon, P.S. Doyle, Rapid microRNA profiling on encoded gel microparticles, Angew. Chem. Int. Ed. 50 (2011) 2289–2293.
[35] S.C. Chapin, P.S. Doyle, Ultrasensitive multiplexed microRNA quantification on encoded gel microparticles using rolling circle amplification, Anal. Chem. 83 (2011) 7179–7185.
[36] H. Zhang, Y. Liu, X. Fu, L. Yuan, Z. Zhu, Microfluidic bead-based assay for microRNAs using quantum dots as labels and enzymatic amplification, Mikrochim. Acta 182 (2015) 661–669.
[37] R. Ishihara, K. Hasegawa, K. Hosokawa, M. Maeda, Multiplex MicroRNA detection on a power-free microfluidic chip with laminar flow-assisted dendritic amplification, Anal. Sci. 31 (2015) 573–576.
[38] H. Arata, H. Komatsu, K. Hosokawa, M. Maeda, Rapid and sensitive microRNA detection with laminar flow-assisted dendritic amplification on power-free microfluidic chip, PloS One 7 (2012).
[39] H. McArdle, E.M. Jimenez-Mateos, R. Raoof, E. Carthy, D. Boyle, H. ElNaggar, N. Delanty, H. Hamer, M. Dogan, T. Huchtemann, "TORNADO"–Theranostic One-Step RNA Detector; microfluidic disc for the direct detection of microRNA-134 in plasma and cerebrospinal fluid, Sci. Rep. 7 (2017) 1–11.
[40] X. Li, P. Rout, R. Xu, L. Pan, P.B. Tchounwou, Y. Ma, Y.-M. Liu, Quantification of microRNAs by coupling cyclic enzymatic amplification with microfluidic voltage-assisted liquid desorption electrospray ionization mass spectrometry, Anal. Chem. 90 (2018) 13663–13669.
[41] Z. Zou, Y. Liu, L. Xia, Z. Hu, J. Yin, Y. Mu, A multiplex and fast detection platform for microRNAs based on a self-priming microfluidic chip and duplex-specific nuclease, Analyst 146 (2021) 628–635.
[42] H. Cai, J. Parks, T. Wall, M. Stott, A. Stambaugh, K. Alfson, A. Griffiths, R. Mathies, R. Carrion, J. Patterson, Optofluidic analysis system for amplification-free, direct detection of Ebola infection, Sci. Rep. 5 (2015) 1–8.
[43] K.N. Hass, M. Bao, Q. He, L. Liu, J. He, M. Park, P. Qin, K. Du, Integrated micropillar polydimethylsiloxane accurate CRISPR detection system for viral DNA sensing, ACS Omega 5 (2020) 27433–27441.
[44] X. Jiang, C. Zhao, X. Fan, W. Xu, R. Zhang, H. Xu, G. Wu, A DNA-modified hydrogel for simultaneous purification, concentration and detection of targeted cfDNA in human serum, RSC Adv. 9 (2019) 3407–3415.
[45] J. Lee, H. Kim, Y. Heo, Y.K. Yoo, S.I. Han, C. Kim, D. Hur, H. Kim, J.Y. Kang, J. H. Lee, Enhanced paper-based ELISA for simultaneous EVs/exosome isolation and detection using streptavidin agarose-based immobilization, Analyst 145 (2020) 157–164.
[46] Y. Zeng, R. Novak, J. Shuga, M.T. Smith, R.A. Mathies, High-performance single cell genetic analysis using microfluidic emulsion generator arrays, Anal. Chem. 82 (2010) 3183–3190.
[47] L. Cheng, R.A. Sharples, B.J. Scicluna, A.F. Hill, Exosomes provide a protective and enriched source of miRNA for biomarker profiling compared to intracellular and cell-free blood, J. Extracell. Vesicles 3 (2014) 23743.
[48] T. Wang, M. Zhang, D.D. Dreher, Y. Zeng, Ultrasensitive microfluidic solid-phase ELISA using an actuatable microwell-patterned PDMS chip, Lab Chip 13 (2013) 4190–4197.
[49] J. Kim, M. Kang, E.C. Jensen, R.A. Mathies, Lifting gate polydimethylsiloxane microvalves and pumps for microfluidic control, Anal. Chem. 84 (2012) 2067–2071.
[50] L.-X. Yan, X.-F. Huang, Q. Shao, M.-Y. Huang, L. Deng, Q.-L. Wu, Y.-X. Zeng, J.-Y. Shao, MicroRNA miR-21 overexpression in human breast cancer is associated with advanced clinical stage, lymph node metastasis and patient poor prognosis, RNA 14 (2008) 2348–2360.
[51] J.-g. Zhang, J.-j. Wang, F. Zhao, Q. Liu, K. Jiang, G.-h. Yang, MicroRNA-21 (miR-21) represses tumor suppressor PTEN and promotes growth and invasion in non-small cell lung cancer (NSCLC), Clin. Chim. Acta 411 (2010) 846–852.
[52] M. Seike, A. Goto, T. Okano, E.D. Bowman, A.J. Schetter, I. Horikawa, E.A. Mathe, J. Jen, P. Yang, H. Sugimura, MiR-21 is an EGFR-regulated anti-apoptotic factor in

lung cancer in never-smokers, Proc. Natl. Acad. Sci. Unit. States Am. 106 (2009) 12085–12090.
[53] J. Ribas, X. Ni, M. Haffner, E.A. Wentzel, A.H. Salmasi, W.H. Chowdhury, T. A. Kudrolli, S. Yegnasubramanian, J. Luo, R. Rodriguez, miR-21: an androgen receptor–regulated microRNA that promotes hormone-dependent and hormone-independent prostate cancer growth, Canc. Res. 69 (2009) 7165–7169.
[54] M. Dillhoff, J. Liu, W. Frankel, C. Croce, M. Bloomston, MicroRNA-21 is overexpressed in pancreatic cancer and a potential predictor of survival, J. Gastrointest. Surg. 12 (2008) 2171.
[55] O. Slaby, M. Svoboda, P. Fabian, T. Smerdova, D. Knoflickova, M. Bednarikova, R. Nenutil, R. Vyzula, Altered expression of miR-21, miR-31, miR-143 and miR-145 is related to clinicopathologic features of colorectal cancer, Oncology 72 (2007) 397–402.
[56] Z. Zhang, Z. Li, C. Gao, P. Chen, J. Chen, W. Liu, S. Xiao, H. Lu, miR-21 plays a pivotal role in gastric cancer pathogenesis and progression, Lab. Invest. 88 (2008) 1358–1366.
[57] H. Parsa, C.D. Chin, P. Mongkolwisetwara, B.W. Lee, J.J. Wang, S.K. Sia, Effect of volume-and time-based constraints on capture of analytes in microfluidic heterogeneous immunoassays, Lab Chip 8 (2008) 2062–2070.
[58] A.D. Stroock, S.K. Dertinger, A. Ajdari, I. Mezić, H.A. Stone, G.M. Whitesides, Chaotic mixer for microchannels, Science 295 (2002) 647–651.
[59] C.-P. Jen, C.-Y. Wu, Y.-C. Lin, C.-Y. Wu, Design and simulation of the micromixer with chaotic advection in twisted microchannels, Lab Chip 3 (2003) 77–81.
[60] C.Y. Lee, C. Lin, M. Hung, R. Ma, C.H. Tsai, C.H. Lin, L.M. Fu, Experimental and numerical investigation into mixing efficiency of micromixers with different geometric barriers, Mater. Sci. Forum, Trans. Tech. Publ. (2006) 391–396.
[61] R.H. Liu, R. Lenigk, R.L. Druyor-Sanchez, J. Yang, P. Grodzinski, Hybridization enhancement using cavitation microstreaming, Anal. Chem. 75 (2003) 1911–1917.
[62] Z. Yang, S. Matsumoto, H. Goto, M. Matsumoto, R. Maeda, Ultrasonic micromixer for microfluidic systems, Sens. Actuators A Phys. 93 (2001) 266–272.